

# AIAA'87

**AIAA-87-0167**

**Tone Generation by Flow Past  
Deep Wall Cavities**

D. D. Erickson and W. W. Durgin,  
Worcester Polytechnic Institute,  
Worcester, MA

**AIAA 25th Aerospace Sciences Meeting**

January 12-15, 1987/Reno, Nevada

For permission to copy or republish, contact the American Institute of Aeronautics and Astronautics  
1633 Broadway, New York, NY 10019

# TONE GENERATION BY FLOW PAST DEEP WALL CAVITIES

D. D. Erickson\* and W. W. Durgin\*\*  
Worcester Polytechnic Institute  
Worcester, Massachusetts

## Abstract

Flow past deep wall cavities exhibits strong interaction with the standing wave system in the cavity. The shear layer separating the exterior flow from the cavity flow supports instabilities which excite the normal cavity modes. In turn, the cavity wave system reinforces the instabilities. Experimental studies have shown that two distinct instability modes are encountered as the external velocity is increased. The pressure coefficient versus Strouhal number behavior reveals two maxima which correspond to different instability modes of the shear layer. Flow visualization studies have shown that these modes correspond to distinct shear layer vortex structures. At high velocities, single large-scale vortices are formed on the interface. At lower velocities, two vortices are present, simultaneously.

## Nomenclature

AR	Cavity Aspect Ratio
$C_p$	Pressure Coefficient
$d$	Cavity depth
$f$	Fundamental Frequency
$f_n$	Cavity Natural Frequency
$f^*$	Frequency Ratio, $f/f_n$
$L$	Streamwise Cavity Dimension
$P$	Total Pressure
$P_{rms}$	Root-Mean-Square Fluctuating Pressure
SPL	Sound Pressure Level
St	Strouhal Number
$T$	Period (Frequency <sup>-1</sup> )
$U_m$	Mean Approach Velocity
$U_r$	Reduced Velocity, $U_m/f_n d$
$\rho$	Density

## Introduction

High velocity flow past the junction of a cavity with a wall can result in the excitation of depth-mode standing waves in the cavity if the depth is large relative to the width ( $L/d \gg 1$ ). The separating shear layer provides coupling between the free stream flow and the cavity,

where, photographic evidence indicates the formation of large-scale vortices at and near resonance. The vortex formation process results from instability of the shear layer and may be classified as a non-linear fluid mechanical oscillator.<sup>1</sup> The wave system formed in the cavity is essentially a standing wave system of nearly linear character. The principle interaction takes place through the excitation of the quarter wavelength mode. Apparently, the shear layer oscillator drives the acoustic oscillator which, in turn, has the ability to control the shear layer through a presently unknown feedback mechanism. The system exhibits bandwidth synchronization in that the shear layer frequency is captured by the depth-mode resonance of the cavity although the resonant response can cause departures of up to  $\pm 10\%$ .

Studies were performed in a sub-sonic wind tunnel using a cavity of fixed cross section and of variable depth. The analysis consisted of two parts. First, the acoustic response was measured at selected cavity depths and exterior flow velocities<sup>2</sup>. Second, flow visualization was employed to study shear layer structures at peak resonant response. These studies are similar to those of Maguire<sup>3</sup> and reported by Erickson et al<sup>4</sup>, utilizing a pipe side-branch configuration.

## Experiments

Experiments were performed in a sub-sonic, open circuit wind tunnel capable of speeds up to 80 m/s. The tunnel had a rectangular test section which measured 45 cm high, 61 cm wide and 91 cm long. A square side-branch cavity was mounted perpendicular to the bottom side of the test section. The side-branch cavity consisted of a 6 cm square cross section with an adjustable depth from 0 cm to 60 cm. A schematic of the wind tunnel is provided in Figure 1.

Power spectra were obtained by fixing the cavity at selected depths ranging from 15 cm to 50 cm and varying the free stream velocity from 30 m/s to 70 m/s.

A power spectrum of the microphone signal was obtained for each cavity length and velocity setting. Non-dimensionalization of the data resulted in the collapse of all data to a generalized plot of pressure coefficient and Strouhal number defined by equations 1 and 2 respectively,

$$C_p = P_{rms} / (1/2 \rho U_m^2) \quad (1)$$

$$St = f_n d / U_m \quad (2)$$

\* Research Assistant, Department of Mechanical Engineering, Student Member AIAA.

\*\* Professor, Department of Mechanical Eng., Member AIAA.

Flow visualization was accomplished by introducing oil vapor smoke into the shear layer, illuminating the smoke with a high intensity strobe lamp and simultaneously obtaining an exposure at a selected time increment in the cycle of the oscillating shear layer. The shear layer was photographed at Strouhal numbers of 0.3 and 0.8 which corresponded to different modes of cavity response. The lower mode of cavity response occurred at a Strouhal number of 0.3, which, for a cavity depth of 25 cm corresponded to a free stream velocity of 60 m/s. The higher mode of cavity response occurred at a Strouhal number of 0.8. Thus, for a cavity depth of 15 cm the free stream velocity was 33 m/s. For each cavity depth, sequential photographs of the shear layer were obtained. Each sequence corresponded to a  $T/8$  increment of the shear layer cycle, where  $T$  is the period of oscillation. Due to the recycle time of the strobe lamp, however, each photograph was a number of integral cycles past the previous photograph.

### Results

Increasing the velocity of exterior flow past a cavity of fixed depth resulted in increasing and then decreasing sound pressure levels. This behavior was observed to occur in two velocity ranges within the limitations of the wind tunnel. Typical power spectra for a 35 cm deep cavity are shown in Figures 2(a) to 2(i). The natural frequency of this cavity was 230 Hz, for the quarter wavelength mode. For a velocity of 30 m/s the cavity response was 125 dB at 205 Hz (a). With the velocity at 40 m/s the peak response occurred at 225 Hz and was 150 dB (b). The largest cavity SPL occurred at 50 m/s and was 159 dB at 225 Hz (c). For velocities of 58 m/s and 61 m/s the cavity frequency remained at 235 Hz and the cavity SPL dropped from 150 dB to 13 dB respectively (d&e). The peak response frequency shifted to the second overtone, at 705 Hz, for velocities of 65 m/s and 67 m/s (f&g). At the second overtone the cavity SPL was 141 dB for 65 m/s (f) and for 67 m/s the response was 138 dB (g). The fundamental frequency was 240 Hz at a SPL of 132 dB for 65 m/s (f), and at 67 m/s the fundamental peak occurred at 245 Hz with a cavity response of 127 dB (g). At 70 m/s peak cavity response occurred at 240 Hz and was 124 dB (h). At the highest velocity, 73 m/s, the cavity response was 125 dB at 235 Hz (i). It is evident, for a cavity depth of 35 cm, that in the velocity range from 30 m/s to 60 m/s the dominant frequency of cavity response was the quarter-mode fundamental. In the velocity range greater than 60 m/s but less than 67 m/s peak cavity response occurred at the second overtone, although a large response still existed at the fundamental. Also it is apparent that the fundamental frequency exhibited a slight dependence on reduced velocity at and near cavity resonance.

Figures 3(a) and 3(b) illustrate the dependence of the fundamental frequency and pressure coefficient on reduced velocity for a 35 cm deep cavity. Over the whole range of reduced velocity, from 2.00 to 5.00, the fundamental frequency did not vary more than  $\pm 11$  percent from the natural frequency of the cavity (a). Over the range of reduced velocity from 2.75 to 4.20 the frequency ratio remained essentially constant ( $f^* = 0.98 \pm .02$ ) and the pressure coefficient ( $C_p$ ) rose to a maximum of 1.17 (b). This region of reduced

velocity corresponded to the strongest coupling between the shear layer and the cavity, often referred to as the region of "lock-on". Considering the resolution of the dynamic signal analyzer, which was  $\pm 5$  Hz, the frequency was essentially "locked" to the cavity mode in this range of  $U_r$ . For reduced velocity beyond 4.2 the frequency continued to rise while the pressure coefficient decreased in magnitude.

Figure 4, a plot of the logarithm of pressure coefficient versus Strouhal number illustrates the response of fixed aspect ratio cavities to increasing velocity. The variation of pressure coefficient with Strouhal number shows two distinct maxima. The greatest response occurred in the range of Strouhal number from 0.3 to 0.4. In this region the cavity pressure excursions were of the order of the free stream dynamic pressure, indicating strong resonance. This maxima corresponded to the lower mode of cavity response and shear layer instability (revealed by flow visualization). A second maxima occurred in the range of Strouhal number from 0.75 to 0.85. Pressure excursions in this region were approximately 40 percent of the free stream dynamic pressure. This region corresponded to a higher mode of shear layer instability (revealed by flow visualization) and lower amplitudes of resonance.

Photographs of the shear layer are shown in Figure 5 for a 25 cm cavity. This sequence of exposures correspond to one "apparent" cycle of the shear layer oscillation. Although each photograph was taken at even increments ( $T/8$ ) of time from the zero crossings of the pressure signal, each is many integral cycles apart. Initially, it is apparent that the vortex structure began to form as the shear layer was deflected into the cavity (a). The vortex grew in diameter as it traveled downstream and impinged on the downstream wall of the cavity (b-e). Subsequently, the shear layer was deflected outward from the cavity, expelling the vortex (f-h). The most striking feature of this process was the scale of the interface motion, which was of the order of the cavity's streamwise dimension. This cycle of events corresponded to a Strouhal number of 0.33 or a cavity frequency of 312 Hz. This process is representative of the lower mode of shear layer instability.

Figure 6 is a similar sequence of photographs of the shear layer in the higher mode of instability. In this mode it is apparent that two vortices were simultaneously formed on the interface. Individually, double vortices followed a history of formation, collision and expulsion similar to that of the single vortex process. Initially a vortex structure formed as the shear layer was deflected into the cavity (a). The vortex was convected along the interface (b) while a second vortex was formed as the primary vortex approached the downstream wall (c). The second vortex continued along the interface as the primary vortex impinged on the downstream wall and was expelled from the cavity (d). Figures 6 (e) to 6 (h) show a similar cycle of this mode of shear layer behavior. The cavity depth was set to 18 cm and the free stream velocity was 33 m/s. The resulting Strouhal number was 0.8 or a cavity frequency of 425 Hz.

### Conclusions

High velocity flow past a deep wall cavity causes substantial tone generation by virtue of the interaction of the shear layer with the resonant cavity. The frequency of the oscillation is essentially determined by the natural frequency (quarter wavelength) of the cavity. The fundamental frequency increases with increasing reduced velocity and "locks" to the natural frequency of the cavity during resonance. The amplitude of response is a function of the reduced velocity. Apparently, the feedback mechanism is such that for lower velocities a double vortex structure exists on the interface and drives the cavity flow at its resonant frequency. At higher velocities it is evident that feedback from the resonant cavity occurs such that a single vortex is formed on the interface. The lower shear layer mode typically results in the strongest coupling and hence larger responses. In both cases the coupling is such that strong reinforcement of the shear layer modes occur.

### References

- 1) Rockwell, D. and Naudascher, E., "Review - Self-Sustaining Oscillations of Flow Past Cavities", ASME J. of Fluids Engineering, Vol. 100, June 1978.
- 2) Lustenberger, P.U., "Feedback Mechanisms in Unstable Flow Past Deep Cavities", M.S. Thesis, Worcester Polytechnic Institute, April, 1985.
- 3) Maguire III, C.F., "An Experimental Investigation of Self-Sustaining Cavity Oscillations in a Pipe Mounted Side-Branch", M.S. Thesis, Worcester Polytechnic Institute, April, 1985.
- 4) Erickson, D.D. et al, "Shear Layer Coupling with Side-Branch Resonators." Transaction Proceedings, Forum on Unsteady Flows, ASME Winter Annual Meeting, 1986.

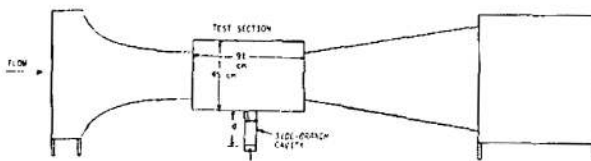


Figure 1  
Wind Tunnel

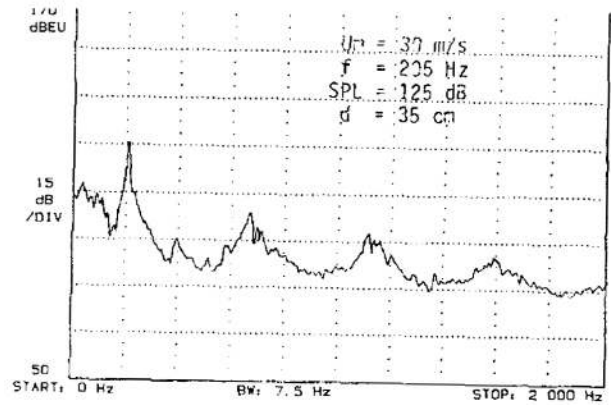


Figure 2a Power Spectra for 35 cm Cavity

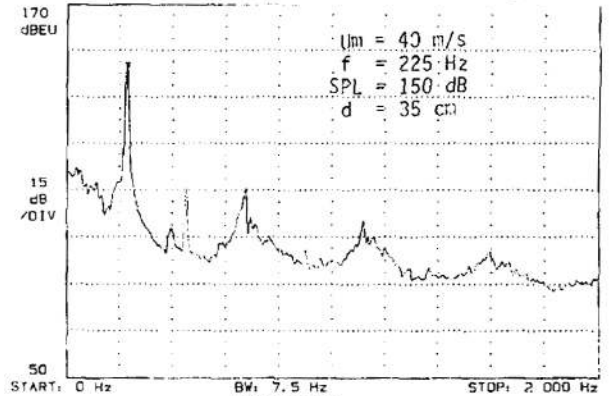


Figure 2b

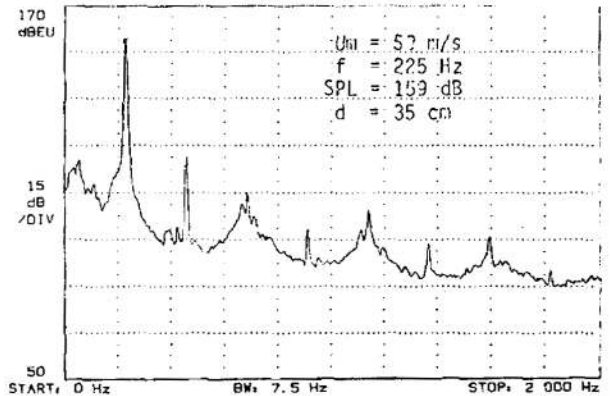


Figure 2c

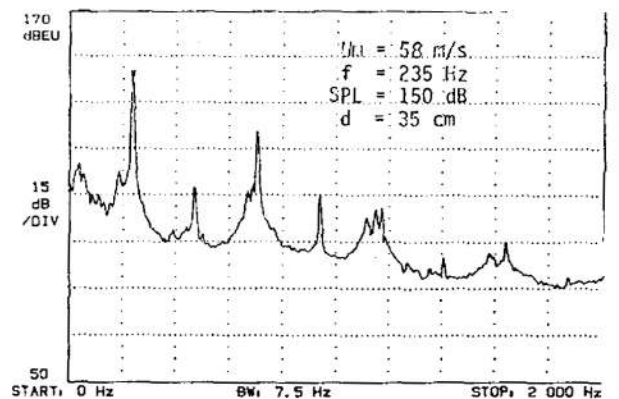


Figure 2d

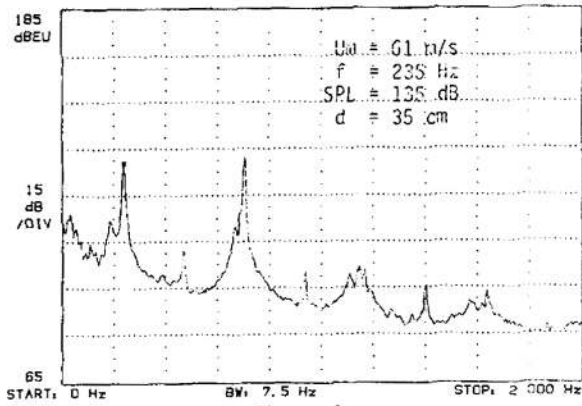


Figure 2e

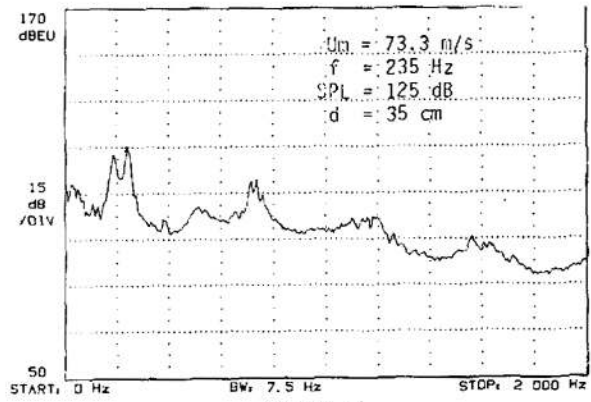


Figure 2i

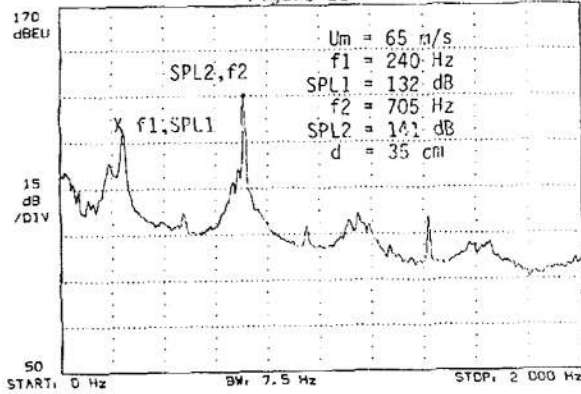


Figure 2f

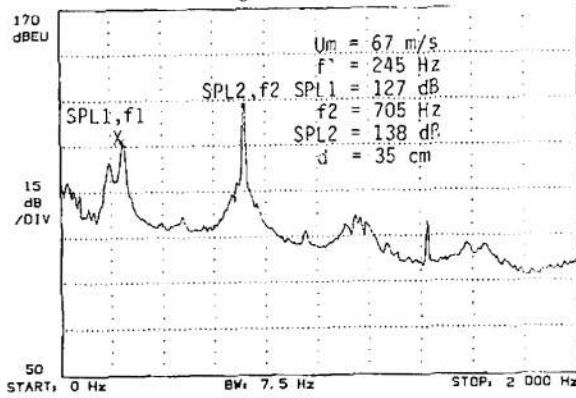


Figure 2g

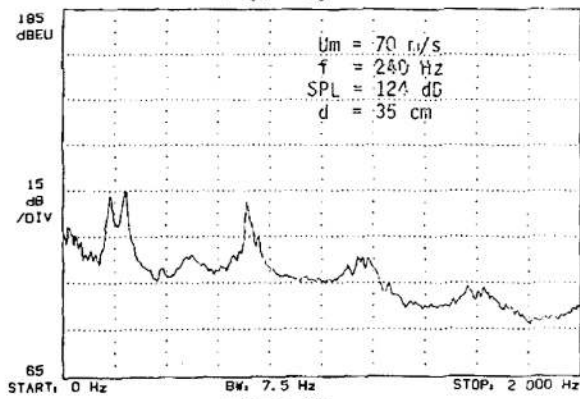


Figure 2h

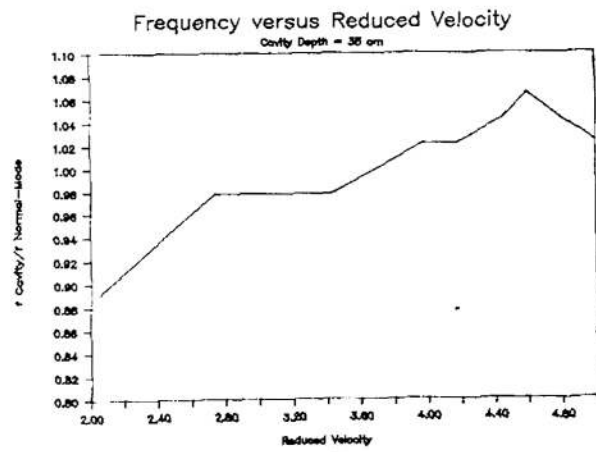


Figure 3a  
Frequency Ratio vs.  
Reduced Velocity

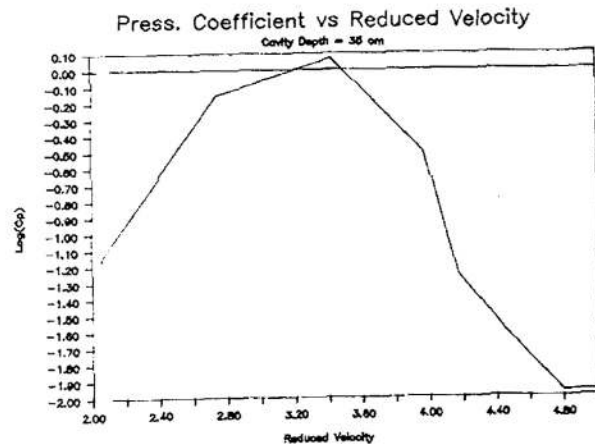


Figure 3b  
Pressure Coefficient vs.  
Reduced Velocity

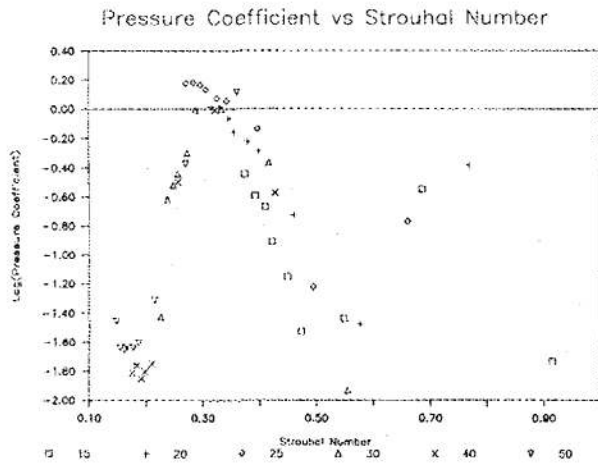


Figure 4 Press. Coeff. vs. Strouhal Number

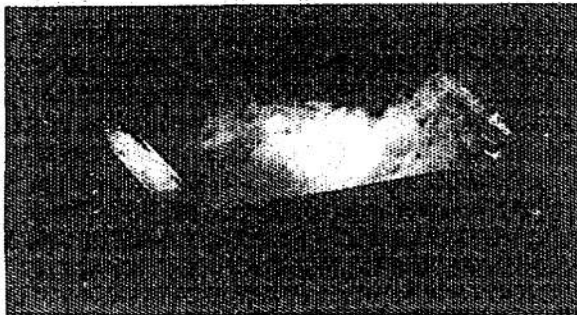


Figure 5a Single Vortex Mode, at  $t = 0$

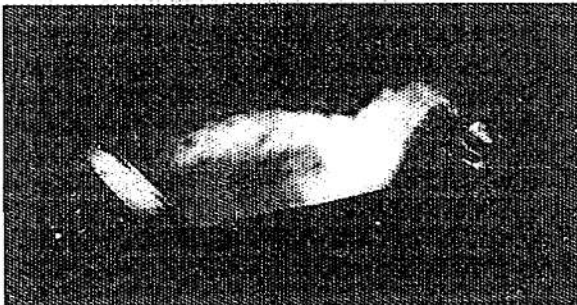


Figure 5b Single Vortex Mode, at  $t = 1/8$

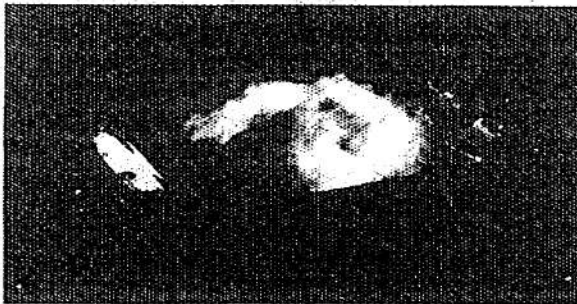


Figure 5c Single Vortex Mode, at  $t = 2/8$

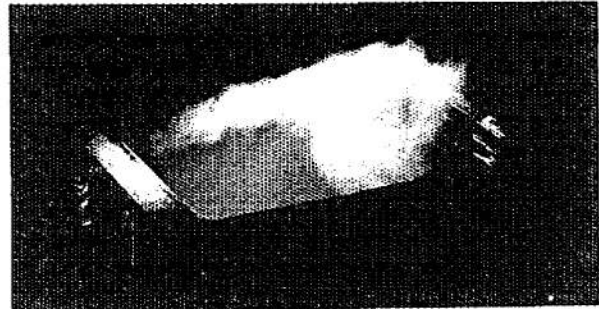


Figure 5d Single Vortex Mode, at  $t = 3/8$



Figure 5e Single Vortex Mode, at  $t = 4/8$



Figure 5f Single Vortex Mode, at  $t = 5/8$

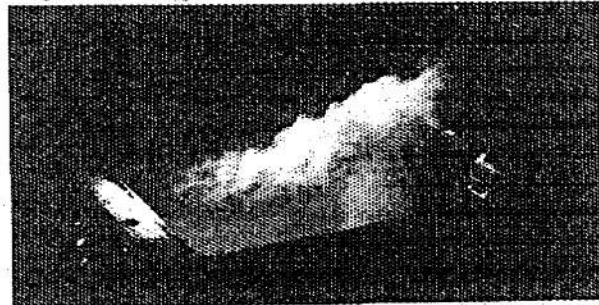


Figure 5g Single Vortex Mode, at  $t = 6/8$



Figure 5h Single Vortex Mode, at  $t = 7/8$



Figure 6a Double Vortex Mode,  $t = 0$



Figure 6e Double Vortex Mode,  $t = 4/8$

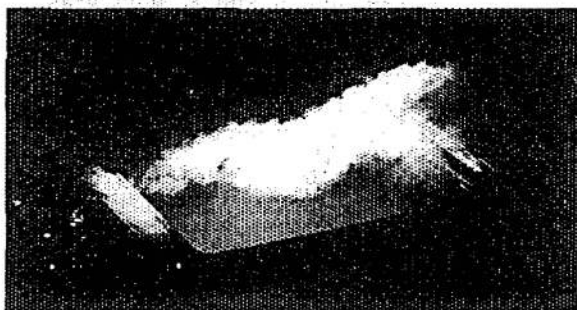


Figure 6b Double Vortex Mode,  $t = 1/8$

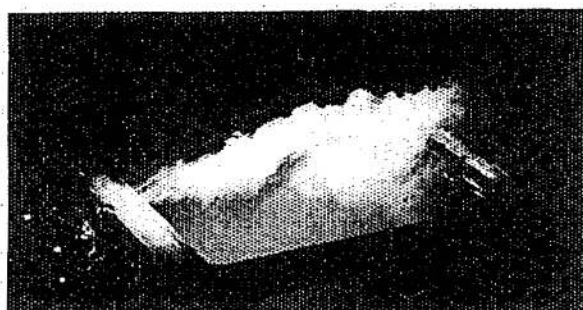


Figure 6f Double Vortex Mode,  $t = 5/8$



Figure 6c Double Vortex Mode,  $t = 2/8$



Figure 6g Double Vortex Mode,  $t = 6/8$



Figure 6d Double Vortex Mode,  $t = 3/8$

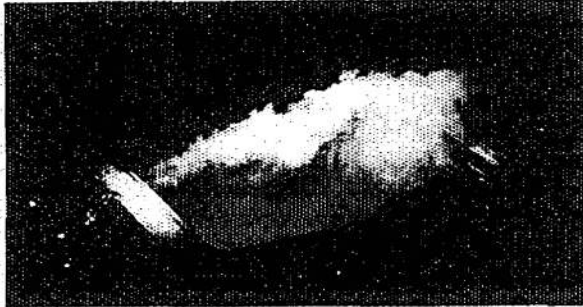


Figure 6h Double Vortex Mode,  $t = 7/8$